

Review

# The Application of Mineral Kaolinite for Environment Decontamination: A Review

Meijuan Chen<sup>1,2,3</sup>, Tongxi Yang<sup>2,3</sup>, Jichang Han<sup>1,\*</sup>, Yang Zhang<sup>1,2,3</sup>, Liyun Zhao<sup>2,3</sup>, Jinghan Zhao<sup>2,3</sup>, Rong Li<sup>4</sup>, Yu Huang<sup>4,\*</sup>, Zhaolin Gu<sup>2,3</sup> and Jixian Wu<sup>2,3</sup>

<sup>1</sup> Key Laboratory of Degraded and Unused Land Consolidation Engineering, The Ministry of Natural Resources of China, Xi'an 710075, China

<sup>2</sup> Technology Innovation Center for Land Engineering and Human Settlements by Shaanxi Land Engineering Construction Group Co., Ltd. and Xi'an Jiaotong University, Xi'an 710049, China

<sup>3</sup> School of Human Settlements and Civil Engineering, Xi'an Jiaotong University, Xi'an 710049, China

<sup>4</sup> Key Lab of Aerosol Chemistry and Physics, State Key Laboratory of Loess and Quaternary Geology (SKLLQG), Institute of Earth Environment, Chinese Academy of Sciences, Xi'an 710061, China

\* Correspondence: hanjc\_sxdj@126.com (J.H.); huangyu@ieecas.cn (Y.H.)

**Abstract:** Kaolinite clay mineral with a layered silicate structure is an abundant resource in China. Due to its advantages of excellent stability, high specific surface area and environmental friendliness, kaolinite is widely used in environment decontamination. By using kaolinite as a carrier, the photocatalytic technology in pure photocatalysts of poor activities, narrow spectral responses, and limited electron transport can be overcome, and the nano-Ag disinfectant's limitation of the growth and aggregation of nanoparticles is released. Moreover, pure kaolinite used as an adsorbent shows poor surface hydroxyl activity and low cation exchange, leading to the poor adsorption selectivity and easy desorption of heavy metals. Current modification methods including heat treatment, acid modification, metal modification, inorganic salt modification, and organic modification are carried out to obtain better adsorption performance. This review systematically summarizes the application of kaolinite-based nanomaterials in environmental decontamination, such as photocatalytic pollutant degradation and disinfection, nano silver (Ag) disinfection, and heavy metal adsorption. In addition, applications on gas phase pollutant, such as carbon dioxide (CO<sub>2</sub>), capture and the removal of volatile organic compounds (VOCs) are also discussed. This study is the first comprehensive summary of the application of kaolinite in the environmental field. The review also illustrates the efficiency and mechanisms of coupling naturally/modified kaolinite with nanomaterials, and the limitation of the current use of kaolinite.

**Keywords:** kaolinite; environment decontamination; photocatalytic degradation; disinfection; adsorption



**Citation:** Chen, M.; Yang, T.; Han, J.; Zhang, Y.; Zhao, L.; Zhao, J.; Li, R.; Huang, Y.; Gu, Z.; Wu, J. The Application of Mineral Kaolinite for Environment Decontamination: A Review. *Catalysts* **2023**, *13*, 123. <https://doi.org/10.3390/catal13010123>

Academic Editor: Giuseppe Mele

Received: 11 December 2022

Revised: 31 December 2022

Accepted: 2 January 2023

Published: 5 January 2023



**Copyright:** © 2023 by the authors. Licensee MDPI, Basel, Switzerland. This article is an open access article distributed under the terms and conditions of the Creative Commons Attribution (CC BY) license (<https://creativecommons.org/licenses/by/4.0/>).

## 1. Introduction

Kaolinite is an abundant clay mineral resource with a layered silicate structure, which is yielded from the natural alteration of feldspar and other silicate minerals. It is a kind of aluminosilicate formed with Al-(O, OH) octahedrons and Si-O tetrahedrons bonded by common oxygen. Kaolinite possesses the advantages of excellent stability, high specific surface area, and environmental friendliness. Moreover, China is a country with rich amounts of kaolinite, with an estimated reserve of 14.3 billion tons. Therefore, kaolinite is competitive and can be used as potential materials for the decontamination of environmental pollutants, especially regarding water treatment and air pollution control. It is often used as a photocatalyst for organic pollutants, adsorbent for heavy metals, CO<sub>2</sub> capture, and removal of VOCs.

Photocatalytic technology is extensively studied using nano-semiconductors such as TiO<sub>2</sub> and ZnO nanostructures. However, these pure nanostructures suffer from poor

activities, narrow spectral responses, and limited electron transport, which restrains the real applications in environmental decontamination. Kaolinite is an optimal candidate to act as nanomaterials' carrier because it has the advantages of low cost, rich reserves, recyclability, and high adsorption capacity [1–3]. In order to boost the generation of active radicals under light from the range of ultraviolet (UV) to visible light and improve the photocatalytic performance on environment decontamination [4], kaolinite has been combined with nano-photocatalysts to synthesize composite materials, such as TiO<sub>2</sub> (titanium dioxide)/kaolinite [5–7], ZnO (zinc oxide)/kaolinite [8,9], g-C<sub>3</sub>N<sub>4</sub> (graphitic carbon nitrides)/kaolinite [10,11], and g-C<sub>3</sub>N<sub>4</sub>/TiO<sub>2</sub>/kaolinite [9,12]. For example, the deposition TiO<sub>2</sub> nanoparticles on the kaolinite carrier (TiO<sub>2</sub>/kaolinite composite) promoted the dispersion of TiO<sub>2</sub> nanoparticles, which benefited the transportation of photoinduced carriers and improved the photocatalytic performance towards the degradation of ciprofloxacin [5]. The g-C<sub>3</sub>N<sub>4</sub> growth on kaolinite (g-C<sub>3</sub>N<sub>4</sub>/kaolinite composite) gave g-C<sub>3</sub>N<sub>4</sub> pore structure and rich reactive sites, which showed better photocatalytic performance than pure g-C<sub>3</sub>N<sub>4</sub> [3].

Ag nanoparticle is a disinfection agent towards bacteria, fungi, algae and viruses, due to the ability of Ag to interact with DNA and thiol-containing proteins after it transports across the cell membrane. However, the practical application of Ag nanoparticles is limited because disinfection technology based on nanomaterials has limitations such as the growth of nanocrystal, the aggregation of nanoparticles, and the changing of the surface morphology, which hampers the disinfection performance and ultimately restrains its real application. Kaolinite is a suitable candidate for the immobilization of Ag nanoparticles to construct nano-Ag/kaolinite composite with well dispersed nanoparticles and improved disinfection performance. Moreover, the recovery and reuse of Ag/kaolinite is easier (especially in water environment), which overcomes the problem of secondary pollution caused by pure Ag nanoparticles [13].

Kaolinite is also an adsorbent for environmental pollutants. It could work as an adsorbent for heavy metals of Cd(II), Fe(III), Co(II) and Ni(II) [14–16]. However, the low cation exchange capacity and specific surface area limit the removal efficiency of pure kaolinite [14]. Therefore, researches have made great efforts to increase the specific surface area, produce a large number of pore structures, and change the surface property of kaolinite. Thermal modification, acid modification, transition metal modification, and organic modification are all efficient methodologies for improving its adsorption of heavy metals [15,17].

This review provides comprehensive information on recent progress in the development and synthesis of kaolinite-based materials. This review systematically summarizes the application of kaolinite-based nanomaterials in environmental decontamination, such as photocatalytic degradation, nano silver (Ag) disinfection, photocatalytic disinfection, and heavy metal adsorption. In addition, the application of kaolinite in gas phase pollutant removal, such as CO<sub>2</sub> reduction and volatile organic compounds (VOCs) degradation, are also discussed. This is the first comprehensive summary of the application of kaolinite in the environmental field. This review also illustrates the efficiency and mechanisms of coupling naturally/modified kaolinite with nanomaterials, and the limitation of the current use of kaolinite.

## 2. The Properties of Kaolinite

The molecular formula of kaolinite is Si<sub>2</sub>AlO<sub>5</sub>(OH)<sub>4</sub>. It consists of 39.50% Al<sub>2</sub>O<sub>3</sub>, 46.54% SiO<sub>2</sub>, and 13.96% H<sub>2</sub>O. Kaolinite is an aqueous aluminosilicate mineral composed of the Al-centered octahedra ([Al<sub>2</sub>(OH)<sub>4</sub>]<sup>2+</sup>) and the Si-centered tetrahedra (Si<sub>2</sub>O<sub>5</sub><sup>2-</sup>) in a two-dimensional arrangement. The crystal structure of kaolinite offers a certain degree of charge non-parallelism because both the Al-centered octahedral layer and the Si-centered tetrahedral layer are negatively charged [18]. Therefore, the oxygen atoms connect the charge-repulsive Al-centered octahedra and Si-centered tetrahedra, and form the layered structure of kaolinite, which promotes the formation of hydrogen bonds to tightly bond kaolinite (Figure 1). Therefore, an abundance of the hydroxyl group is supplied on the

surface of kaolinite, which is active group and benefits the further chemical treatment, including anchoring nanoparticles (such as TiO<sub>2</sub>, ZnO, g-C<sub>3</sub>N<sub>4</sub>, Ag) and surface modification (such as thermal-modified kaolinite, acid-modified kaolinite, transition metal-modified kaolinite, and organic-modified kaolinite).

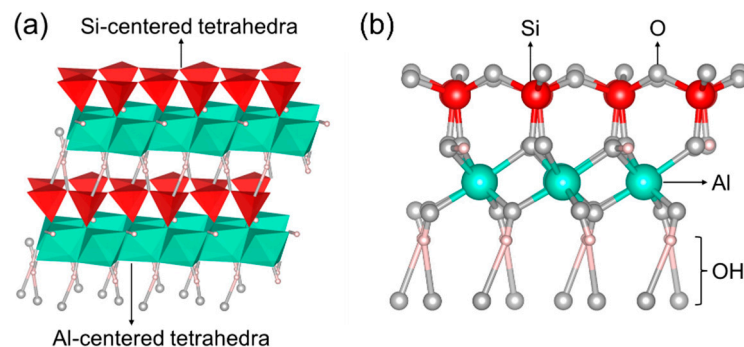


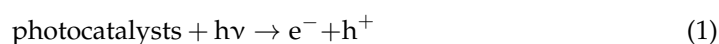
**Figure 1.** The structure model (a), and the stick model (b) of kaolinite. (The red color represents Si component, the blue color represents Al component, the gray ball is O atom, and the pink ball is H atom).

### 3. Photocatalytic Degradation of Organic Pollutions

Aqueous organic pollutants can cause serious harm to human health and the ecological environment. Traditional wastewater treatment processes of coagulation, sedimentation, filtration, and biological treatment have the disadvantages of non-recyclability, high cost, and low efficiency [19,20]. In contrast, photocatalytic degradation is a promising technology with extensive applications for the direct harvesting and conversion of the solar energy to generate active radicals for the pollutants' degradation [21,22]. Because the nanostructures in pure, such as ZnO, TiO<sub>2</sub>, and g-C<sub>3</sub>N<sub>4</sub>, suffer from poor activities, narrow spectral responses, and limited electron transport, kaolinite can be used as a carrier for nano-photocatalysts to generate synergistic effects, including promoting dispersion of nano-photocatalysts, increasing the pollutants' contact with surface active components, and enhancing the restorability, which significantly improves the photocatalytic degradation performance [1,10].

#### 3.1. Photocatalysis Mechanism

The reactive species of photocatalytic degradation of organic pollutants in semiconductor materials mainly includes photogenerated holes (h<sup>+</sup>), superoxide radicals (O<sub>2</sub><sup>·-</sup>), and hydroxyl radicals (HO·). When light with wavelengths below the absorption threshold of the semiconductor is used, the semiconductor produces photogenerated electrons (e<sup>-</sup>) and h<sup>+</sup> (Equation (1)). In addition, e<sup>-</sup> are generated from the conduction band (CB) of the semiconductor and h<sup>+</sup> are generated from the valence band (VB); e<sup>-</sup> react with O<sub>2</sub> to generate O<sub>2</sub><sup>·-</sup> (Equation (2)), and h<sup>+</sup> are captured by hydroxyl groups to generate HO· in aqueous solution (Equation (3)). Then, the formed h<sup>+</sup>, O<sub>2</sub><sup>·-</sup>, and HO· act as oxidants to interact with organic pollutants, which finally degrade into small molecules such as CO<sub>2</sub>, H<sub>2</sub>O, and inorganic acids [4,9,23]. The schematic illustration of the photocatalytic reaction mechanism is shown in Figure 2 [22].



The high adsorption capacity and excellent sedimentation performance of kaolinite make it an ideal carrier for photocatalytic semiconductor materials, thus it is widely used in organic pollutants such as pharmaceuticals, personal care products (PPCPs), and

dyes [24]. In this section, the applications of different kaolinite-based photocatalysts in the degradation of organic pollutants are summarized.

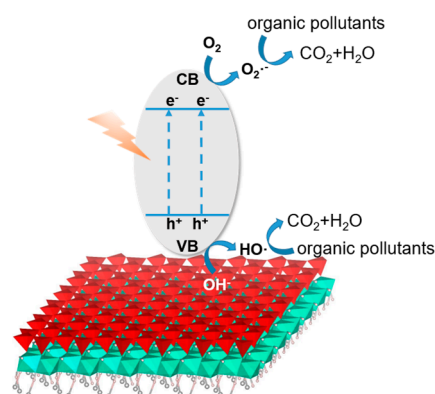


**Figure 2.** Schematic illustration of photocatalytic reaction mechanism.

### 3.2. $\text{TiO}_2$ /Kaolinite Photocatalysis

Despite the fact that semiconductor  $\text{TiO}_2$  has been reported as possessing the advantages of simple and mild synthesis conditions and excellent photo-corrosion resistance, its photocatalytic ability is not high because of its limited specific surface area. Coating  $\text{TiO}_2$  on the surface of kaolinite is an efficient way to increase the specific surface area. Li et al. [25] synthesized a  $\text{TiO}_2$ /kaolinite photocatalyst by using a simple sol-gel method. The synthesized  $\text{TiO}_2$ /kaolinite was 1.42 times higher than the pure  $\text{TiO}_2$ . Moreover, the degradation rate constant of the prepared  $\text{TiO}_2$ /kaolinite is 7.90 times higher than pure  $\text{TiO}_2$ , ascribing to the introduction of micropores and mesopores, which enhanced the adsorption, diffusion, and desorption of organic pollutant ciprofloxacin in the composite, and further increased the photocatalytic degradation performance. In addition, this research found that the calcination temperature for  $\text{TiO}_2$ /kaolinite preparation is a key factor for affecting the specific surface area. When the calcination temperature increased from 105 to 300 °C, the specific surface area of the  $\text{TiO}_2$ /kaolinite increased from 74.77 to 106.19  $\text{m}^2/\text{g}$ , resulting in an increased decay efficiency from 82.72% to 92.4%. However, when the calcination temperature was beyond 300 °C, the photocatalytic performance dramatically decreased to 60.26%, accompanied by the specific surface area's decrease to 74.77  $\text{m}^2/\text{g}$ . The decline of the specific surface area is mainly attributed to the damage and collapse of the micropore structure caused by the exceeded calcination temperature. Another  $\text{TiO}_2$ /kaolinite photocatalyst prepared by hydrothermal method [26] showed that its specific surface area and average pore volume increased 15.1 fold and 2.1 fold, respectively, compared to pure  $\text{TiO}_2$ . As a result, the photocatalytic degradation efficiency on dye RhB reached 99.51% in 120 min, which was better than the pure  $\text{TiO}_2$  of 88.35%. The specific surface area and photocatalytic degradation performance were also affected by the morphologies of kaolinite [27]. Li et al. [28] prepared  $\text{TiO}_2$ /kaolinite by adjusting the kaolinite morphologies to nanoflake- and nanorod-like. The  $\text{TiO}_2$  nanoparticles/nanoflake-like kaolinite achieve a higher tetracycline hydrochloride degradation efficiency of 98% than  $\text{TiO}_2$  nanoparticles/nanorod-like kaolinite (84%), pure  $\text{TiO}_2$  (10%), and pure kaolinite (20%). Compared to the small specific surface area of pure  $\text{TiO}_2$  nanoparticles ( $S_{\text{BET}} = 13 \text{ m}^2/\text{g}$ ), the specific surface area of  $\text{TiO}_2$  nanoparticles/nanorod-like kaolinite and  $\text{TiO}_2$  nanoparticles/nanoflake-like kaolinite increased to 109  $\text{m}^2/\text{g}$  and 114  $\text{m}^2/\text{g}$ , respectively, which promoted the dispersion of  $\text{TiO}_2$ .

Because  $\text{TiO}_2$  is a wide band gap material and absorbs only in the UV region, another efficient way to enhance the photocatalytic performance is to explore the light absorption to visible light. Wang et al. [29] fabricated broadened light absorption  $\text{TiO}_2$ /kaolinite composites by using the titanium tetrachloride ( $\text{TiCl}_4$ ) hydrolysis method, where the kaolinite played a key role in the crystal phase transformation because it promoted the growth of anatase  $\text{TiO}_2$  by inhibiting the transformation of the anatase phase to the rutile phase. Consequently, the light absorption was increased with absorption edge shifting

from 400 nm to 417 nm, and the photocatalytic performance on dye methyl orange was improved.

Surface modification of TiO<sub>2</sub>/kaolinite photocatalysts by changing the surface properties of kaolinite is effective in improving the degradation performance. Xu et al. [30] synthesized TiO<sub>2</sub>/kaolinite composites by using HCl acid-treated kaolinite as a carrier. After acid treatment on kaolinite, hydroxyl groups were introduced on the surface of kaolinite, which offered more sites for loading TiO<sub>2</sub> grains, resulting in an enhanced performance of 93.94% on the organic dye methylene blue, compared to the 77.71% at the untreated kaolinite. Oliveira et al. [20] applied H<sub>2</sub>SO<sub>4</sub> to alter the surface property of TiO<sub>2</sub> and kaolinite, which positively charged TiO<sub>2</sub> and negatively charged kaolinite. The electrostatic attraction promoted the interaction between TiO<sub>2</sub> and kaolinite. Therefore, the degradation performance of organic dye methylene blue followed the order of H<sub>2</sub>SO<sub>4</sub> acid treated TiO<sub>2</sub>/kaolinite > TiO<sub>2</sub>/kaolinite > TiO<sub>2</sub>.

### 3.3. Other Semiconductor/Kaolinite Photocatalysis

Other photocatalytic semiconductors, such as ZnO, g-C<sub>3</sub>N<sub>4</sub>, and bismuth oxychloride (BiOCl), were also used for loading on the kaolinite carrier. The morphologies of kaolinite affected the specific surface area and thereby the photocatalytic degradation performance of the ZnO/kaolinite and g-C<sub>3</sub>N<sub>4</sub>/kaolinite composites. Kutlákova et al. used a simple hydrothermal method to synthesize the ZnO/kaolinite composites [31]. Its decay efficiency of dye acid orange 7 reached 95%. Abukhadra et al. [32] revealed that the morphology of kaolinite showed an important influence on the photocatalytic performance. The ZnO/nanotube-like kaolinite showed a 99% levofloxacin (an organic pollutant) degradation rate, which was 76.7% higher than that of ZnO/bulk kaolinite. This is because the higher specific surface area of kaolinite nanotubes benefited the formation of homogeneous ZnO nanoparticles and further enhanced the light absorption capacity. A two-dimensional lamellar g-C<sub>3</sub>N<sub>4</sub>/kaolinite composite was synthesized and its apparent rate constant on photocatalytic degradation of dye RhB is 2.1 times higher than that of bare g-C<sub>3</sub>N<sub>4</sub> because the two-dimensional lamellar structure offered tight interfacial bonding between g-C<sub>3</sub>N<sub>4</sub> and kaolinite, and benefited the separation of the photogenerated electron-hole pairs [9]. Furthermore, the treatment of kaolinite by cyanuric acid led to the generation of abundant pore structures and reactive sites. As a result, the apparent rate constant of cyanuric acid modified g-C<sub>3</sub>N<sub>4</sub>/kaolinite is 1.9 times than that of g-C<sub>3</sub>N<sub>4</sub>/kaolinite. In addition, Sun et al. [3] found that the loading amount of g-C<sub>3</sub>N<sub>4</sub> significantly affected the photocatalytic performance of the g-C<sub>3</sub>N<sub>4</sub>/kaolinite composites, where the optimum loading amount was determined as 40% (mass ratios of g-C<sub>3</sub>N<sub>4</sub> with respect to kaolinite) because it presented the higher adsorption capacity on RhB. Considering the fact that the photocatalytic reaction always occurred on the catalyst surface [33], the higher adsorption of RhB led to the better degradation performance. Moreover, the good dispersity of g-C<sub>3</sub>N<sub>4</sub> on the g-C<sub>3</sub>N<sub>4</sub>/kaolinite composite promoted the separation of photogenerated electrons and holes, providing more reactive radicals for RhB degradation [3].

### 3.4. Dual Semiconductor-Based Kaolinite Photocatalysis

Despite being above the single semiconductor TiO<sub>2</sub>, ZnO and g-C<sub>3</sub>N<sub>4</sub> based kaolinite composites showed good performance on organic pollutant decay, but they still suffered from narrow spectral response and limited electron transport, which exhibited limited degradation rates for organic pollutants [34]. Dual semiconductors-based kaolinite composites provided an efficient way to alleviate the aforementioned limitations [4]. Li et al. [35] constructed a g-C<sub>3</sub>N<sub>4</sub>-TiO<sub>2</sub> heterojunction supported on kaolinite (g-C<sub>3</sub>N<sub>4</sub>-TiO<sub>2</sub>/kaolinite) to accelerate the internal charges' separation. The g-C<sub>3</sub>N<sub>4</sub>-TiO<sub>2</sub>/kaolinite had an enhanced visible light absorption region with a band gap of 2.72 eV and an enhanced photocatalytic removal efficiency for ciprofloxacin, showing an apparent rate constant 5.35 times than that of pure TiO<sub>2</sub>, and 6.35 times than that of g-C<sub>3</sub>N<sub>4</sub>. The ternary g-C<sub>3</sub>N<sub>4</sub>-TiO<sub>2</sub>/kaolinite composite had a looser porous structure, higher specific surface area, and smaller TiO<sub>2</sub>

grain size, which facilitated the adsorption, migration, and degradation of the organic pollutant ciprofloxacin. Huang et al. [36] prepared a ternary cerium dioxide ( $\text{CeO}_2$ )/g- $\text{C}_3\text{N}_4$ /kaolinite composite via combining the sol-gel and hydrothermal method. Compared with the decay efficiency of pure  $\text{CeO}_2$  (42%) and g- $\text{C}_3\text{N}_4$  (51%), the ternary  $\text{CeO}_2$ /g- $\text{C}_3\text{N}_4$ /kaolinite composite showed an enhanced degradation efficiency (90%) on the organic pollutant. The superior performance of the ternary composite was attributed to its larger specific surface area, lower band gap, and bigger pore volume. Dong et al. [10] introduced g- $\text{C}_3\text{N}_4$  and BiOCl on kaolinite carrier to form a ternary BiOCl/g- $\text{C}_3\text{N}_4$ /kaolinite composite. The use of BiOCl increased the light absorption intensity in the visible light range, and further enhanced the photocurrent and the interface charge transfer. As a result, the degradation rate on RhB by BiOCl/g- $\text{C}_3\text{N}_4$ /kaolinite is 10 times that of g- $\text{C}_3\text{N}_4$ /kaolinite and 5.5 times that of BiOCl.

#### 4. Disinfection with Ag Materials and Photocatalysis

##### 4.1. Disinfection with Ag Materials

Pathogenic microorganisms present a serious threat to human and animal health especially in the aqueous environment [37]. Ag nanoparticle is a disinfection agent towards bacteria, fungi, algae, and viruses because Ag can interact with DNA and thiol-containing proteins after passing through the cell membrane. However, Ag nanoparticles are easy to aggregate owing to van der Waals forces and the high surface energy of nanoparticles, which limits its practical application. Constructing the Ag nanoparticles on the kaolinite surface can solve these problems. E. Ward et al. [38] prepared a Ag/kaolinite composite that showed good antibacterial and antifungal activity, in which the incorporation of Ag nanoparticles into a kaolinite carrier retarded the aggregation of the Ag nanoparticles. Furthermore, to benefit the composites' separation, Woldegebreal et al. [39] synthesized a magnetic  $\text{Fe}_3\text{O}_4$ -Ag/kaolinite composite by introducing the magnetic  $\text{Fe}_3\text{O}_4$  into Ag/kaolinite, which can be easily separated from water after application, and achieved efficient disinfection performance on *Salmonella paratyphi* and *Escherichia coli* bacteria. Moreover, the increment of the loading amount of Ag nanocomposite contributed to a significant enhancement in the disinfection performance with the loading amount increased from 0.1 g to 0.7 g. Apart from combining with the magnetic materials, the combination of the organic antibacterial agent also improved the disinfection performance. Jou's study [40] deposited an organic antibacterial agent, i.e., chlorhexidine acetate, onto the Ag/kaolinite surface to prepare a chlorhexidine-Ag/kaolinite composite with enhanced antibacterial activity, which presented excellent antibacterial activity on both Gram-positive bacteria and Gram-negative bacteria. The antibacterial activity of chlorhexidine-Ag/kaolinite composite was better than Ag/kaolinite and chlorhexidine/kaolinite because it produced a larger total inhibition zone and gave a lower minimum inhibition concentration.

##### 4.2. Disinfection with Photocatalysis

Photocatalytic disinfection is a promising technology for environmental disinfection due to the use of solar energy and no secondary pollution [41–43]. Numerous studies have shown that photocatalytic disinfection can be used to remove a series of bacteria such as *Escherichia coli*, *Staphylococcus aureus*, *Pseudomonas aeruginosa*, and *Enterococcus faecalis*. The mechanism of photocatalytic disinfection is similar to the photocatalytic degradation, where generated radicals such as  $\text{O}_2^{\cdot-}$  and  $\text{HO}\cdot$  via photocatalysis are the main species for the destruction and inactivation of micro-organisms [13]. However, the drawbacks of photocatalytic disinfection with pure photocatalysts are similar to that of photocatalytic pollutant degradation, i.e., poor activities, narrow spectral responses, and limited electron transport. Using kaolinite as the catalyst carrier can alleviate these problems to a certain extent. A  $\text{TiO}_2$ /kaolinite was prepared via sol-gel method and achieved 5 bacterial log-reduction units on *Escherichia coli* sp. (ATCC 11775) under 120 min irradiation, which was superior to the pure  $\text{TiO}_2$  [44]. The operational factors, such as  $\text{TiO}_2$ /kaolinite dosage, pH, and aeration rate, were found showing great impact on disinfection activity. Fatimah

et al. [45] synthesized TiO<sub>2</sub>/kaolinite photocatalytic composites, and the photocatalytic disinfection activity on bacterial *Escherichia coli* achieved 100%. This antibacterial performance was affected by the loading amount of TiO<sub>2</sub> (of kaolinite mass), and the optimum loading amount of TiO<sub>2</sub> is determined as 10% in mass ratio because it gave a higher band gap energy (3.21 eV) with a broadened light absorption spectrum and a larger specific surface area (40.928 m<sup>2</sup>/g).

The TiO<sub>2</sub>/kaolinite only responds to UV light, which hinders its photocatalytic performance under visible light or solar light. Doping is an efficient method to expand the response spectrum to visible light. For example, B. Aritonang et al. [46] prepared a Bi-doped TiO<sub>2</sub>/kaolinite photocatalyst via sol-gel method followed by calcination at 450 °C. With the irradiation of visible light, the prepared Bi-doped TiO<sub>2</sub>/kaolinite showed a higher bacterial inactivation performance on *Escherichia coli* and *Staphylococcus aureus* than TiO<sub>2</sub>/kaolinite composite. This is because the light response was expanded from ultraviolet to visible light, and the band gap significantly decreased from 3.22 eV (TiO<sub>2</sub>) to 2.76 eV (Bi-doped TiO<sub>2</sub>), which originated from the incorporation of Bi<sup>3+</sup> to form Bi-O-Ti bonds. Misra et al. [47] prepared Fe-doped ZnO/kaolinite composites via co-precipitation method, which achieved the highest disinfection efficiency (100%) on multidrug resistant *Enterobacter* sp. under visible light irradiation compared with Fe-doped ZnO and kaolinite. The excellent disinfection efficiency was due to the smaller negative surface charge of Fe-doped ZnO/kaolinite than ZnO and kaolinite, thereby the surface of Fe-doped ZnO/kaolinite composite can interact more closely with the negatively charged *Enterobacter* sp. cell membrane and improve the bactericidal performance. Moreover, the Fe doped in the composite decreased the band gap of the photocatalyst and accelerated the separation of the photogenerated electron and hole [48], thereby increasing the photocatalytic activity. The photocatalytic disinfection performance is greatly affected by the reaction temperature. In Wang's study, when the reaction temperature varied in a range of 35–55 °C, the TiO<sub>2</sub>/kaolinite showed the highest disinfection efficiency at 55 °C because of the faster cell death at higher temperatures [26].

To improve the utilization of solar energy and regulate the rate and path of photo-generated electron and hole pairs, Li et al. fabricated a novel sandwich structure g-C<sub>3</sub>N<sub>4</sub>/TiO<sub>2</sub>/kaolinite composite using a mild sol-gel method, which is an efficient antimicrobial photocatalyst [35]. Under the visible-light irradiation, the sandwich structure g-C<sub>3</sub>N<sub>4</sub>/TiO<sub>2</sub>/kaolinite displayed better disinfection performance on bacterial *S. aureus* than bare g-C<sub>3</sub>N<sub>4</sub>, TiO<sub>2</sub>, and kaolinite. The CuO-ZnO/kaolinite composite synthesized by Ugwuja et al. [49] showed improved efficiency on *E. coli* disinfection compared to CuO/kaolinite and ZnO/kaolinite, because the CuO-ZnO/kaolinite nanocomposite was operated by three disinfecting mechanisms, i.e., electrostatic interaction, metal toxicity of the leaching Zn and Cu, and photocatalysis.

## 5. Adsorption of Heavy Metals

Heavy metal pollution has attracted much attention due to its serious damages to water, air, and soil. Adsorption is one of the most efficient approaches to remove heavy metals from the environment [17,23,50]. Heavy metal adsorbents mainly include carbon materials derived from biological wastes (activated carbon), clay minerals (kaolinite), and so on [4,51]. Therefore, kaolinite possesses research value for the adsorption of heavy metals due to its advantages of having a wide source, low cost, and no secondary pollution to the environment by using the physical adsorption principle [52]. However, kaolinite showed poor performance as an adsorbent to removal heavy metals such as Fe(III), Ni(II), Co(II), and Cd(II) [14,15,53]. To improve the adsorption capacity of kaolinite, different methods such as thermal modification, acid modification, transition metal modification, and organic modification were adopted [54].

### 5.1. Natural Kaolinites

Natural kaolinites show a certain ability to adsorb heavy metals, e.g., Ni(II), Zn(II), and Cu(II). The adsorption performance is affected by operating parameters such as reaction time, solution pH, and temperature. Yavuz et al. [55] removed the heavy metal Ni(II) by using natural kaolinite as an adsorbent. The adsorption of Ni(II) on kaolinite fitted the Langmuir adsorption equation well with a Langmuir constant of Ni(II) of 1.669 mg/g. The adsorption of Ni(II) was significantly affected by the adsorption temperature because adsorption is an endothermic process, and the adsorption rate will be accelerated at high temperatures. Shahmohammadi et al. [56] investigated the removal of Zn(II) by raw kaolinite in aqueous phase. The adsorption capacity for Zn(II) was measured to be 4.95 mg/g, indicating kaolinite is an effective adsorbent to remove Zn(II). Chai et al. [57] studied the adsorption of Zn(II) by kaolinite under different operating conditions. The results revealed that the adsorption equilibrium was achieved in 60 min at 25 °C, the maximum adsorption capacity reached 6.35 mg/g, and the adsorption efficiency exceeded 95%. Chai et al. also pointed out that the mechanism of Zn(II) interaction with kaolinite includes surface complexation, cation exchange, electrostatic attraction, and precipitation. Moreover, the adsorption capacity increased with the increment of the reaction time, the solution pH and the operating temperature. Farsi et al. [58] evaluated the removal of Cu(II) by kaolinite in an aqueous solution. The results revealed that solution pH and operating temperature significantly affect the removal efficiency on Cu(II), i.e., when the pH level increased from 2 to 6, the removal efficiency gradually increased. Moreover, the removal efficiency improved when the operating temperature increased from 25 °C to 35 °C.

However, pure kaolinite showed poor surface hydroxyl activity and low cation exchange, leading to the poor adsorption selectivity and easy desorption of heavy metals, which restrains the practical application of kaolinite. Therefore, researchers are devoted to modifying kaolinite to obtain better performance, and the current modification methods for kaolinite mainly include heat treatment, acid modification, metal modification, inorganic salt modification, and organic modification [59].

### 5.2. Thermal-Modified Kaolinite

Thermal modification refers to the heating of kaolinite at a certain temperature so as to effectively remove H<sub>2</sub>O molecules, carbonates, and other organic impurities attached to the pore structure of kaolinite [60]. The disappearance of different forms of water molecules such as adsorbed water, crystalline water, and structural water can effectively increase the specific surface area and the pore volume of kaolinite, and the removal of structural water will transform it into metakaolinite, which exposes it to the generation of a large number of sites for reaction with acid. Meanwhile, its activity is enhanced and easily reacts with acid, which eventually improves the ion exchange performance and adsorption performance of kaolinite for pollutants [61]. Yan et al. [62] converted natural kaolinite into amorphous metakaolinite through a simple thermal activation method, leading to the removal of structural water in kaolinite, and formed two-dimensional sheet morphology with the increased surface area. TiO<sub>2</sub> was then attached to the thermal activation kaolinite to prepare a highly dispersed and stable TiO<sub>2</sub>/modified kaolinite composite, which was used as an adsorbent to remove Pb(II). The result showed that the highly dispersed titanium species on the surface of the composite could react with the exposed hydroxyl groups in kaolinite to form the titanium hydroxyl groups. The strong bond connection between the formed titanium hydroxyl groups and Pb(II) caused the high adsorption capacity of Pb(II). It was known that the high hydrophobicity of TiO<sub>2</sub> restrained its real application in water purification. In comparison, the modified kaolinite is hydrophilic, thus the TiO<sub>2</sub> dispersed on the modified kaolinite gave a hydrophobicity–hydrophilicity balance. Therefore, the Pb(II) adsorption capacities via TiO<sub>2</sub>/modified kaolinite composite (184 mg/g) were much higher than the modified kaolinite (64 mg/g). Bhattacharyya [15] reported that a thermal modified kaolinite prepared by calcination at 600 °C was efficient for the adsorption of

heavy metals (Pb(II), Cd(II), and Cu(II)) because the calcination at the high temperature brought out the collapsed kaolinite, giving rise to the porous structure on kaolinite.

### 5.3. Acid-Modified Kaolinite

Acid modification refers to the pretreatment of kaolinite by organic or inorganic acids to remove impurities carried by kaolinite itself [63]. Acid modification of kaolinite not only increases the surface acidity and specific surface area of kaolinite, but also results in the production of a large number of pore structures [64]. Bhattacharyya and Gupta [65] treated kaolinite with H<sub>2</sub>SO<sub>4</sub> to further improve its properties. The modified kaolinite with H<sub>2</sub>SO<sub>4</sub> opened the edges of kaolinite sheet crystals, resulting in the increased pore size and the enlarged specific surface area, and the adsorption rate constant of kaolinite for Cu(II) increased from  $9.5 \times 10^{-2}$  g/mg·min to  $12.0 \times 10^{-2}$  g/mg·min. Chai et al. [66] prepared an acid-activated kaolinite by refluxing the kaolinite in the concentrated H<sub>2</sub>SO<sub>4</sub> solution. This H<sub>2</sub>SO<sub>4</sub> activated kaolinite showed excellent adsorption performance on both Ni(II) and Cu(II). Moreover, the H<sub>2</sub>SO<sub>4</sub> activated kaolinite possessed a higher adsorption capacity than raw kaolinite, and the maximum adsorption capacities of H<sub>2</sub>SO<sub>4</sub> activated kaolinite towards Ni(II) and Cu(II) achieved 39.62 mg/g and 41.11 mg/g, respectively, while the adsorption capacity of raw kaolinite was slightly lower, showing 37.64 mg/g for Ni(II) and 40.01 mg/g for Cu(II), respectively. The improvement in the H<sub>2</sub>SO<sub>4</sub> activated kaolinite should be ascribed to two reasons. First, the acid-activated kaolinite became smaller in size and appeared to be disintegrated, which increased the specific surface area by 84.58%. Second, the acid treatment with H<sub>2</sub>SO<sub>4</sub> changed the surface property of kaolinite, such as the number of effective binding sites and surface negative charges. Unuabonah et al. [67] prepared a humic-acid-modified kaolinite and used it for the adsorption of several heavy metals, including Pb(II), Cd(II), Zn(II), Ni(II), and Cu(II). It was found that using humic acid for kaolinite modification partially increased the total charges on the kaolinite surface, which further increased the cation exchange capacity. Therefore, the adsorption capacity of the humic-acid-modified kaolinite on heavy metals was increased.

### 5.4. Co-Modified Kaolinite with Thermal Treatment and Acid Treatment

Although thermal modification and acid modification alone can enhance the properties of kaolinite, previous studies revealed that the co-modified kaolinite by both thermal modification and acid modification showed higher microporous volume and specific surface area than the sole [68]. Abdallah [69] modified the kaolinite with acid treatment with 2 mol/L HCl followed by a heating treatment at 600 °C. The co-modification increased the adsorption properties of natural kaolinites by enhancing the cation exchange capacities. The crystal structure of kaolinite transformed to a collapsed structure after being co-modified with acid treatment and thermal treatment, and the collapsed kaolinite possessed a large number of porous structures, which assisted in the massive adsorption of heavy metals Zn(II) and Cu(II) from wastewater. Moreover, the co-modified kaolinite showed a lower Zn(II) adsorption than Cu(II) because when the Zn(II) desorbed into the solution, it could be combined with the chloride ions to form a stable chloride complex, which could not be re-adsorbed by the co-modified kaolinite.

### 5.5. Transition Metal-Modified Kaolinite

Transition metal modification can introduce transition metals between kaolinite layers or on the surface to protonate the surface and broaden the application range of kaolinite; because the transition metal ions are positively charged, they have strong electrostatic attraction and ligand exchange with the negatively charged natural kaolinite minerals [70]. Ç. Üzümlü et al. [71] synthesized zero-valent iron (nZVI) with kaolinite (nZVI/Kaolinite), which showed a significant effect on the iso-electric point. The iso-electric point for the natural kaolinite and the nZVI/kaolinite is pH 4.2 and 7.0, respectively. Therefore, the nZVI/kaolinite is more suitable for removing heavy metals at environmental pH levels. Moreover, the adsorption capacity of Cu(II) is obviously related to the modified amount

of nZVI in the nZVI/kaolinite composite, where the removal capacity on Cu(II) increased from 32 mg/g to 140 mg/g as the mass ratio of nZVI/kaolinite increased from 0.2/1 to 1/1. However, the uptake capacity of Co(II) increased slightly from 23 mg/g to 25 mg/g. This different adsorption performance was explained by the removal of Co(II), which was determined through adsorption and precipitation, while the removal of Cu(II) was mainly attributed to a reduction reaction with zero valent iron, leading to the insoluble Cu<sub>2</sub>O and Cu(0) phases. Modified kaolinite with aluminum sulphate (Al<sub>2</sub>(SO<sub>4</sub>)<sub>3</sub>) [72] was carried out as adsorbents (Al<sub>2</sub>(SO<sub>4</sub>)<sub>3</sub>/kaolinite) to remove heavy metal Pb(II) from the aqueous phase. It was found that the adsorbed amount of Pb(II) with Al<sub>2</sub>(SO<sub>4</sub>)<sub>3</sub>/kaolinite was 4.5-fold higher than that of raw kaolinite. This is because the layers of kaolinite were broken after the modification, leading to the formation of nano/microsized particles with a big surface area. Moreover, ion exchange was another important mechanism for Pb(II) removal. The kaolinite modification with Al<sub>2</sub>(SO<sub>4</sub>)<sub>3</sub> (Al<sub>2</sub>(SO<sub>4</sub>)<sub>3</sub>/kaolinite) improved the ion exchange capacity because the cation exchange capacity of the Al<sub>2</sub>(SO<sub>4</sub>)<sub>3</sub>/kaolinite is 2.5 times that of the raw kaolinite. Ahmet Sari et al. [73] investigated the adsorption efficiency of MnO<sub>2</sub>/kaolinite for the removal of cadmium ions Cd(II) from waste water. The results revealed that a Mn-OH group was formed by the introduction of MnO<sub>2</sub>, thus the adsorption of Cd(II) was mainly carried out through chemical ion exchange. Moreover, the higher negative charge density of MnO<sub>2</sub> generated on the modified kaolinite surface increased its adsorption capacity, where the adsorption capacities of MnO<sub>2</sub>/kaolinite and kaolinite for Cd(II) were 36.47 and 14.11 mg/g, respectively. Egirani et al. [74] modified the kaolinite with copper oxide (CuO/kaolinite) via the titration method and then used it on Pb(II) removal from water. The modification with CuO gave a good adsorption on Pb(II) because the Pb(II) adsorption by CuO/kaolinite was mainly controlled by the reorganization of active sites. Abou-El-Sherbini et al. [75] explored a ZrO<sub>2</sub>/kaolinite adsorbent for the Cd(II) removal. The insertion of ZrO<sub>2</sub> improved the laminar packing of kaolinite and created new micropores, which increased the specific surface area by 250%. As a result, the adsorption performance of ZrO<sub>2</sub>/kaolinite was three times higher than that of unmodified kaolinite.

### 5.6. Organic-Modified Kaolinite

Inorganic salt modification improved the adsorption properties of kaolinite via changing the surface morphology and the stretching vibrations of Al-O and Si-O bonds without destroying the crystal structure of kaolinite [76]. There are still limitations in some of the modified methods mentioned above, especially acid modification, which may lead to structural decomposition of kaolinite and thus affect the adsorption of heavy metals through some groups located at the edges of kaolinite [77]. Therefore, these drawbacks have accelerated the research on the organic modification of kaolinite, which can impart different surface properties to clay minerals depending on the type and nature of the loaded organic functional groups [78]. Organic modifications are often used to modify kaolinite with polymers, surfactants, and other organic substances [79]. These organic modifications enable the introduction of highly reactive groups, such as -SH and -NH<sub>2</sub>, attaching to the surface of kaolinite, resulting in high adsorption capacity and unique selectivity for heavy metals [80]. Bhattacharyya and Gupta studied the removal of Cu(II) from the aqueous solution [81]; in order to improve the adsorption performance on Cu(II), tetrabutylammonium (TBA) was used to modify kaolinite, and the intercalation of TBA formed a porous skeleton in kaolinite. The specific surface area of TBA/kaolinite was 3.7 times that of the raw kaolinite. E.I. Unuabonah et al. [82] synthesized a polyvinyl alcohol (PVA) modified kaolinite (PVA/kaolinite) with excellent adsorption capacity on heavy metals Pb<sup>2+</sup> and Cd<sup>2+</sup> as the adsorption capacity of the PVA/kaolinite increased to 29.85 mg/g, which was six times higher than that of unmodified kaolinite. Anna Koteja et al. [83] obtained organically modified kaolinite by replacing the intercalation layers with diethanolamine (DEA) and triethanolamine (TEA). It was found that the modified kaolinite with both DEA and TEA showed higher adsorption capacity on the heavy metals of Zn(II), Cd(II), Cu(II), and Pb(II) than the unmodified kaolinite.

## 6. Removal of Gas Phase Pollutants

Apart from the application of kaolinite in photocatalytic pollutant degradation, disinfection, and adsorption, it still presents some applications in air pollutants, such as carbon dioxide (CO<sub>2</sub>) capture, the removal of volatile organic compounds (VOCs), etc. In this part, the applications on the gas phase pollutants of CO<sub>2</sub> capture and the VOCs thermal catalysis are summarized.

### 6.1. CO<sub>2</sub> Reduction and Adsorption

The combustion of fossil fuels leads to the increase of CO<sub>2</sub> content in the atmosphere and intensifies the greenhouse effect. Therefore, reducing CO<sub>2</sub> to avoid greenhouse effect is the focus of current research. CO<sub>2</sub> photocatalytic reduction refers to the use of light to simulate a photosynthesis system. First, CO<sub>2</sub> is adsorbed on the catalyst, then electron hole pairs are generated and separated. Subsequently, it reacts with CO<sub>2</sub> and H<sub>2</sub>O adsorbed on the photocatalyst surface, and is finally converted into green and pollution-free substances such as methane and methanol. The use of kaolinite as a carrier for the photocatalyst can reduce CO<sub>2</sub> to hydrocarbons. Kočí et al. [84] prepared a TiO<sub>2</sub>/kaolinite composite via hot solution method. It was found that the grain size of TiO<sub>2</sub> decreased when it deposited on the surface of kaolinite, leading to the fast transport of photogenerated electrons and holes and making the yield of methane and methanol produced by CO<sub>2</sub> photocatalytic higher than that of commercial TiO<sub>2</sub>. Reli et al. [85] also found that the CO<sub>2</sub> photocatalytic reduction yield by TiO<sub>2</sub>/kaolinite composites was affected by the size of TiO<sub>2</sub> nanocrystals. The calcination temperature and duration time in the TiO<sub>2</sub>/kaolinite catalyst preparation significantly influenced the grain size of TiO<sub>2</sub>. Moreover, the reduction efficiency of CO<sub>2</sub> was the highest when the TiO<sub>2</sub> grain size was smaller than 18–23 nm. Knížek et al. [86] modified the TiO<sub>2</sub>/kaolinite through the addition of HCl, creating a clear edge with a band gap of 2.8 eV in the UV-vis reflectance spectrum, thus offering the HCl modified kaolinite a certain degree of photocatalytic ability on CO<sub>2</sub> reduction. Chen et al. [87] synthesized g-C<sub>3</sub>N<sub>4</sub>/kaolinite composites via an in-situ synthesis method. The g-C<sub>3</sub>N<sub>4</sub>/kaolinite presented the specific surface area of 61.9 m<sup>2</sup>/g, which is three times larger than that of raw kaolinite, originating from the intercalation reactions that occurred between the kaolinite and melamine (g-C<sub>3</sub>N<sub>4</sub> precursor). This augment increases the active sites' number and the charge transfer. Therefore, the photocatalytic activity of the g-C<sub>3</sub>N<sub>4</sub>/kaolinite was better than bare g-C<sub>3</sub>N<sub>4</sub> and kaolinite.

Schaef et al. [88] studied the adsorption of CO<sub>2</sub> onto kaolinite using density functional theory (DFT) methods, which suggested that the interactions between CO<sub>2</sub> and the kaolinite surface resulted in the increase of CO<sub>2</sub> adsorption to 0.34 g/cm<sup>3</sup>. A previous study proved that Al in the electronic structure of kaolinite could be replaced by other elements to change its adsorption capacity for CO<sub>2</sub> [89]. Hou et al. [90] calculated the variation of electronic structures when the Al element in kaolinite was substituted by Si element, indicating that the Si dopant induced a strong interaction between kaolinite and CO<sub>2</sub>, which led to a significant enhancement on the adsorption capacity of CO<sub>2</sub>. This improvement benefited from the small radius of Si ion, and the distance between the kaolinite and CO<sub>2</sub> became shorter after replacing.

### 6.2. Removal of VOCs by Adsorption, Photocatalysis, and Catalytic Combustion

In recent decades, with the fast application and development in industry, VOCs have received widespread attention due to their serious impact on atmospheric environmental pollution and human health [91]. Kaolinite is also often used as a carrier or to prepare component sub-sieves to remove VOCs.

The porous structure of kaolinite provides a big surface area for VOC adsorption. Liu et al. [92] reported that the kaolinite showed excellent methane adsorption performance compared to other clay minerals such as montmorillonite and illite. Heller et al. [93] revealed that the factors affecting the maximum adsorption capacity of kaolinite were the specific surface area and the amount of adsorbed water. Deng et al. [94] found that the ad-

sorption of benzene mainly occurred on the external surface of kaolinite. The procedure of heating kaolinite at 120 °C increased the adsorption of benzene because the adsorption active sites occupied by H<sub>2</sub>O molecules were exposed by heating, and the specific surface area was increased accordingly. Lain et al. [95] found that the kaolinite could selectively remove toluene and phenol in the atmosphere. The results revealed that its adsorption of toluene (−68.2 kJ/mol) and phenol (−87.1 kJ/mol) is stronger than that of CO<sub>2</sub> (−35.0 kJ/mol) and H<sub>2</sub>O (−62.4 kJ/mol). Swasy et al. [96] prepared a polyethylenimine-functionalized kaolinite to adsorb butyric acid, butyraldehyde, and dimethyl disulfide vapor. The raw kaolinite was poor in the remediation of these VOCs. Fortunately, the polyethylenimine-functionalized kaolinite showed an excellent ability on VOC capture, and the removal efficiency for butyraldehyde, dimethyl disulfide, and butyric acid reached 100%, 99%, and 90%, respectively.

Dong et al. [10] prepared a “sandwich” structured BiOCl/g-C<sub>3</sub>N<sub>4</sub>/kaolinite composite by fixing g-C<sub>3</sub>N<sub>4</sub> and BiOCl layer by layer on the kaolinite surface, which showed a high formaldehyde photodegradation efficiency of 74.55% under visible light. This “sandwich” heterojunction built the close interface contact among BiOCl, g-C<sub>3</sub>N<sub>4</sub>, and kaolinite, which effectively promoted the transport and separation of photogenerated electron and hole pairs, and enhanced the photodegradability on formaldehyde. Mora et al. [97] prepared the TiO<sub>2</sub>/kaolinite and used it as a photocatalyst in the degradation of VOCs' toluene. The study showed that the thermal treatment on TiO<sub>2</sub>/kaolinite by calcination at 400 °C was an effective approach to improve the toluene degradation performance (up to 90%) because the thermal treatment strongly affected the structural evolution by changing the clay from kaolinite to metakaolinite, and TiO<sub>2</sub> was in an anatase phase at 400 °C. Kibanova et al. [98] prepared a TiO<sub>2</sub>/kaolinite composite using the sol-gel method and examined the photocatalytic efficiency for the removal of toluene and d-limonene, which exhibited a comparable photocatalytic performance to the commercial TiO<sub>2</sub> (Degussa P25). A CeO<sub>2</sub>-MnO<sub>x</sub>/kaolinite [99] was prepared and showed an excellent thermal-catalytic property on benzene. The molar ratio of Mn/Ce significantly affected the activity for benzene combustion. Among different Mn/Ce ratios, the Mn/Ce = 9:1 showed the highest catalytic degradation performance on benzene, and the benzene could be completely oxidized at 260 °C. Moreover, the performance was kept almost constant via a continuous reaction of 800 h. The good thermal-catalytic performance of the CeO<sub>2</sub>-MnO<sub>x</sub>/kaolinite mainly originated from the well dispersion of CeO<sub>2</sub> nanoparticles on the catalyst surface, and the high oxidation state of MnO<sub>x</sub>.

## 7. Conclusions and Perspective

Kaolinite is a rich mineral in China. Its advantages of being low-cost, non-toxic, environmentally friendly, and stable make it a good candidate for a carrier or adsorbent of environment decontamination. In this review, the utilization of kaolinite as the photocatalysts' carrier was investigated by constructing the ZnO/kaolinite, g-C<sub>3</sub>N<sub>4</sub>/kaolinite, g-C<sub>3</sub>N<sub>4</sub>-TiO<sub>2</sub>/kaolinite, and CeO<sub>2</sub>-g-C<sub>3</sub>N<sub>4</sub>/kaolinite composites. Their synthesized methods, photocatalytic performance, and the intrinsic mechanisms were deeply discussed for organic pollutant degradation and disinfection. The efficient approaches for enhancing the photocatalytic performance included increasing the specific surface area, expanding the light absorption from UV light to visible light, changing the surface properties of kaolinite, and so on. In addition, we analyzed the application of kaolinite as a carrier for nano Ag disinfection. The adjustment of the morphology of Ag/kaolinite, combined with the functions of magnetic and organic antibacterial agents, also significantly improved the disinfection performance. Moreover, kaolinite can be used as an adsorbent for heavy metal removal. The removal performance was improved by thermal modification, acid modification, transition metal modification, and organic modification. Finally, a few applications in CO<sub>2</sub> capture and VOC removal were considered.

Despite a few valuable studies based on kaolinite being reported, the application of kaolinite as a carrier for nano-catalyst and nano-disinfectant, as well as an adsorbent, is

still in the primary stage and needs to be further improved. In addition, the application of kaolinite in industry is still limited because the modification of kaolinite is difficult to achieve. In order to better solve the problem of environmental decontamination and alleviate the crisis of energy supply, the research on kaolinite-based composites should focus on the following aspects: (1) The photocatalytic mechanism of the synergistic effect between photocatalysts and kaolinite should be deeply investigated. (2) It is better to find convenient methods to grow Ag nanoparticles in the interlayer of the layered structured kaolinite, which can effectively control the size and prevent the agglomeration of Ag nanoparticles. (3) Using the modified kaolinite as an absorbent only cannot meet the needs of actual heavy metal removal. Therefore, the effective combination of kaolinite with other treatment processes should be used to satisfy the demand. (4) Future efforts should focus on synthesizing kaolinite-based materials with energy saving and low-cost methods.

**Author Contributions:** Conceptualization, M.C., Y.Z., J.H. and Z.G.; methodology, T.Y., L.Z. and J.Z.; writing—original draft preparation, M.C., T.Y., L.Z., J.Z. and J.W.; writing, M.C., T.Y., L.Z. and R.L.; supervision, Y.H. and Z.G.; project administration, Y.Z., J.H. and Z.G.; funding acquisition, M.C. All authors have read and agreed to the published version of the manuscript. The contributions of the Key Laboratory of Degraded and Unused Land Consolidation Engineering and Xi'an Jiaotong University are equal.

**Funding:** This work was funded by the National Science Foundation of China (No. 41877481), the Opening Fund of Key Laboratory of Degraded and Unused Land Consolidation Engineering, the Ministry of Natural Resources (No. SZDJ2019-15), the Opening Fund of Key Laboratory of Aerosol Chemistry and Physics, Institute of Earth Environment, CAS (No. KLACP2002).

**Data Availability Statement:** Not applicable.

**Conflicts of Interest:** The authors declare no conflict of interest.

## References

1. Akkari, M.; Aranda, P.; Ben Rhaiem, H.; Ben Haj Amara, A.; Ruiz-Hitzky, E. ZnO/clay nanoarchitectures: Synthesis, characterization and evaluation as photocatalysts. *Appl. Clay Sci.* **2016**, *131*, 131–139. [\[CrossRef\]](#)
2. Ma, J.; Huang, D.; Zhang, W.; Zou, J.; Kong, Y.; Zhu, J.; Komarneni, S. Nanocomposite of exfoliated bentonite/g-C<sub>3</sub>N<sub>4</sub>/Ag<sub>3</sub>PO<sub>4</sub> for enhanced visible-light photocatalytic decomposition of Rhodamine B. *Chemosphere* **2016**, *162*, 269–276. [\[CrossRef\]](#) [\[PubMed\]](#)
3. Sun, Z.; Yao, G.; Zhang, X.; Zheng, S.; Frost, R.L. Enhanced visible-light photocatalytic activity of kaolinite/g-C<sub>3</sub>N<sub>4</sub> composite synthesized via mechanochemical treatment. *Appl. Clay Sci.* **2016**, *129*, 7–14. [\[CrossRef\]](#)
4. Chen, Z.; Wei, W.; Chen, H.; Ni, B.J.E.-E. Recent advances in waste-derived functional materials for wastewater remediation. *Eco-Environ. Health* **2022**, *1*, 86–104. [\[CrossRef\]](#)
5. Dědková, K.; Matějová, K.; Lang, J.; Peikertová, P.; Kutláková, K.M.; Neuwirthová, L.; Frydryšek, K.; Kukutschová, J. Antibacterial activity of kaolinite/nanoTiO<sub>2</sub> composites in relation to irradiation time. *J. Photochem. Photobiol. B* **2014**, *135*, 17–22. [\[CrossRef\]](#) [\[PubMed\]](#)
6. Fatimah, I.; Sahroni, I.; Putra, H.P.; Rifky Nugraha, M.; Hasanah, U.A. Ceramic membrane based on TiO<sub>2</sub>-modified kaolinite as a low cost material for water filtration. *Appl. Clay Sci.* **2015**, *118*, 207–211. [\[CrossRef\]](#)
7. Hai, Y.; Li, X.; Wu, H.; Zhao, S.; Deligeer, W.; Asuha, S. Modification of acid-activated kaolinite with TiO<sub>2</sub> and its use for the removal of azo dyes. *Appl. Clay Sci.* **2015**, *114*, 558–567. [\[CrossRef\]](#)
8. García-Giménez, R.; de la Villa, R.V.; Martínez-Ramírez, S.; Fernández-Carrasco, L.; Frías, M. Influence of ZnO on the activation of kaolinite-based coal waste: Pozzolan activity and mineralogy in the pozzolan/lime system. *Appl. Clay Sci.* **2018**, *156*, 202–212. [\[CrossRef\]](#)
9. Sun, Z.; Yuan, F.; Li, X.; Li, C.; Xu, J.; Wang, B. Fabrication of Novel Cyanuric Acid Modified g-C<sub>3</sub>N<sub>4</sub>/Kaolinite Composite with Enhanced Visible Light-Driven Photocatalytic Activity. *Minerals* **2018**, *8*, 437. [\[CrossRef\]](#)
10. Dong, X.; Sun, Z.; Zhang, X.; Li, C.; Zheng, S. Construction of BiOCl/g-C<sub>3</sub>N<sub>4</sub>/kaolinite composite and its enhanced photocatalysis performance under visible-light irradiation. *J. Taiwan Inst. Chem. Eng.* **2018**, *84*, 203–211. [\[CrossRef\]](#)
11. Zhang, C.; Li, Y.; Shuai, D.; Shen, Y.; Xiong, W.; Wang, L. Graphitic carbon nitride (g-C<sub>3</sub>N<sub>4</sub>)-based photocatalysts for water disinfection and microbial control: A review. *Chemosphere* **2019**, *214*, 462–479. [\[CrossRef\]](#)
12. Reli, M.; Huo, P.; Šihor, M.; Ambrožová, N.; Troppová, I.; Matějová, L.; Lang, J.; Svoboda, L.; Kušrowski, P.; Ritz, M.; et al. Novel TiO<sub>2</sub>/C<sub>3</sub>N<sub>4</sub> Photocatalysts for Photocatalytic Reduction of CO<sub>2</sub> and for Photocatalytic Decomposition of N<sub>2</sub>O. *J. Phys. Chem. A* **2016**, *120*, 8564–8573. [\[CrossRef\]](#) [\[PubMed\]](#)
13. Svarovsky, L. 1—Introduction to solid-liquid separation. In *Solid-Liquid Separation*, 4th ed.; Svarovsky, L., Ed.; Butterworth-Heinemann: Oxford, UK, 2001; pp. 1–29. [\[CrossRef\]](#)

14. Adebowale, K.O.; Unuabonah, I.E.; Olu-Owolabi, B.I. The effect of some operating variables on the adsorption of lead and cadmium ions on kaolinite clay. *J. Hazard. Mater.* **2006**, *134*, 130–139. [[CrossRef](#)] [[PubMed](#)]
15. Bhattacharyya, K.G.; Gupta, S.S. Adsorption of a few heavy metals on natural and modified kaolinite and montmorillonite: A review. *Adv. Colloid Interface Sci.* **2008**, *140*, 114–131. [[CrossRef](#)] [[PubMed](#)]
16. Bhattacharyya, K.G.; Gupta, S.S. Kaolinite and montmorillonite as adsorbents for Fe(III), Co(II) and Ni(II) in aqueous medium. *Appl. Clay Sci.* **2008**, *41*, 1–9. [[CrossRef](#)]
17. Zheng, R.; Gao, H.; Ren, Z.; Cen, D.; Chen, Z. Preparation of activated bentonite and its adsorption behavior on oil-soluble green pigment. *Physicochem. Probl. Miner. Process.* **2017**, *53*, 829–845. [[CrossRef](#)]
18. Cao, Z.; Wang, Q.; Cheng, H. Recent advances in kaolinite-based material for photocatalysts. *Chin. Chem. Lett.* **2021**, *32*, 2617–2628. [[CrossRef](#)]
19. Al-Mamun, M.R.; Kader, S.; Islam, M.S.; Khan, M.Z.H. Photocatalytic activity improvement and application of UV-TiO<sub>2</sub> photocatalysis in textile wastewater treatment: A review. *J. Environ. Chem. Eng.* **2019**, *7*, 103248. [[CrossRef](#)]
20. Alfred, M.O.; Omorogie, M.O.; Bodede, O.; Moodley, R.; Ogunlaja, A.; Adeyemi, O.G.; Günter, C.; Taubert, A.; Iermak, I.; Eckert, H. Solar-active clay-TiO<sub>2</sub> nanocomposites prepared via biomass assisted synthesis: Efficient removal of ampicillin, sulfamethoxazole and artemether from water. *Chem. Eng. J.* **2020**, *398*, 125544. [[CrossRef](#)]
21. Wen, J.; Xie, J.; Chen, X.; Li, X. A review on g-C<sub>3</sub>N<sub>4</sub>-based photocatalysts. *Appl. Surf. Sci.* **2017**, *391*, 72–123. [[CrossRef](#)]
22. Dai, W.; Mu, J.; Chen, Z.; Zhang, J.; Pei, X.; Luo, W.; Ni, B.-J.J. Design of few-layer carbon nitride/BiFeO<sub>3</sub> composites for efficient organic pollutant photodegradation. *Environ. Res.* **2022**, *215*, 114190. [[CrossRef](#)]
23. Chen, Z.; Wei, W.; Ni, B.-J.; Chen, H. Plastic wastes derived carbon materials for green energy and sustainable environmental applications. *Environ. Funct. Mater.* **2022**, *1*, 34–48. [[CrossRef](#)]
24. Li, C.; Zhu, N.; Yang, S.; He, X.; Zheng, S.; Sun, Z.; Dionysiou, D.D. A review of clay based photocatalysts: Role of phyllosilicate mineral in interfacial assembly, microstructure control and performance regulation. *Chemosphere* **2021**, *273*, 129723. [[CrossRef](#)]
25. Li, C.; Zhu, N.; Dong, X.; Zhang, X.; Chen, T.; Zheng, S.; Sun, Z. Tuning and controlling photocatalytic performance of TiO<sub>2</sub>/kaolinite composite towards ciprofloxacin: Role of 0D/2D structural assembly. *Adv. Powder Technol.* **2020**, *31*, 1241–1252. [[CrossRef](#)]
26. Azeez, S.O.; Saheed, I.O.; Adekola, F.A.; Salau, S.S. Preparation of TiO<sub>2</sub>-activated kaolinite composite for photocatalytic degradation of rhodamine B dye. *Appl. Clay Sci.* **2011**, *53*, 646–649. [[CrossRef](#)]
27. Bockstaller, M.R.; Mickiewicz, R.A.; Thomas, E.L. Block copolymer nanocomposites: Perspectives for tailored functional materials. *Adv. Mater.* **2005**, *17*, 1331–1349. [[CrossRef](#)]
28. Li, X.; Peng, K.; Chen, H.; Wang, Z. TiO<sub>2</sub> nanoparticles assembled on kaolinites with different morphologies for efficient photocatalytic performance. *Sci. Rep.* **2018**, *8*, 1–11. [[CrossRef](#)]
29. Wang, C.; Shi, H.; Zhang, P.; Li, Y. Synthesis and characterization of kaolinite/TiO<sub>2</sub> nano-photocatalysts. *Appl. Clay Sci.* **2011**, *53*, 646–649. [[CrossRef](#)]
30. Shao, P.; Tian, J.; Yang, F.; Duan, X.; Gao, S.; Shi, W.; Luo, X.; Cui, F.; Luo, S.; Wang, S. Identification and Regulation of Active Sites on Nanodiamonds: Establishing a Highly Efficient Catalytic System for Oxidation of Organic Contaminants. *Adv. Funct. Mater.* **2018**, *28*, 1705295. [[CrossRef](#)]
31. Kutláková, K.M.; Tokarský, J.; Peikertová, P. Functional and eco-friendly nanocomposite kaolinite/ZnO with high photocatalytic activity. *Appl. Catal. B* **2015**, *162*, 392–400. [[CrossRef](#)]
32. Abukhadra, M.R.; Helmy, A.; Sharaf, M.F.; El-Meligy, M.A.; Soliman, A.T.A. Instantaneous oxidation of levofloxacin as toxic pharmaceutical residuals in water using clay nanotubes decorated by ZnO (ZnO/KNTs) as a novel photocatalyst under visible light source. *J. Environ. Manag.* **2020**, *271*, 111019. [[CrossRef](#)]
33. Roy, P.; Jahromi, H.; Adhikari, S.; Finrock, Y.Z.; Rahman, T.; Ahmadi, Z.; Mahjouri-Samani, M.; Feyzbar-Khalkhali-Nejad, F.; Oh, T.-S. Performance of biochar assisted catalysts during hydroprocessing of non-edible vegetable oil: Effect of transition metal source on catalytic activity. *Energy Convers. Manag.* **2022**, *252*, 115131. [[CrossRef](#)]
34. Tong, Z.; Yang, D.; Xiao, T.; Tian, Y.; Jiang, Z. Biomimetic fabrication of g-C<sub>3</sub>N<sub>4</sub>/TiO<sub>2</sub> nanosheets with enhanced photocatalytic activity toward organic pollutant degradation. *Chem. Eng. J.* **2015**, *260*, 117–125. [[CrossRef](#)]
35. Li, C.; Sun, Z.; Zhang, W.; Yu, C.; Zheng, S. Highly efficient g-C<sub>3</sub>N<sub>4</sub>/TiO<sub>2</sub>/kaolinite composite with novel three-dimensional structure and enhanced visible light responding ability towards ciprofloxacin and *S. aureus*. *Appl. Catal. B* **2018**, *220*, 272–282. [[CrossRef](#)]
36. Huang, Z.; Li, L.; Li, Z.; Li, H.; Wu, J. Synthesis of novel kaolin-supported g-C<sub>3</sub>N<sub>4</sub>/CeO<sub>2</sub> composites with enhanced photocatalytic removal of ciprofloxacin. *Materials* **2020**, *13*, 3811. [[CrossRef](#)]
37. Dhandole, L.K.; Kim, S.-G.; Seo, Y.-S.; Mahadik, M.A.; Chung, H.S.; Lee, S.Y.; Choi, S.H.; Cho, M.; Ryu, J.; Jang, J.S. Enhanced Photocatalytic Degradation of Organic Pollutants and Inactivation of *Listeria monocytogenes* by Visible Light Active Rh-Sb Codoped TiO<sub>2</sub> Nanorods. *ACS Sustain. Chem. Eng.* **2018**, *6*, 4302–4315. [[CrossRef](#)]
38. Awad, M.E.; López-Galindo, A.; Medarević, D.; Milenković, M.; Ibrić, S.; El-Rahmany, M.M.; Iborra, C.V. Enhanced antimicrobial activity and physicochemical stability of rapid pyro-fabricated silver-kaolinite nanocomposite. *Int. J. Pharm.* **2021**, *598*, 120372. [[CrossRef](#)] [[PubMed](#)]
39. Woldegebreal, T.; Teju, E.; Kebede, A.; Taddesse, A.; Bezu, Z. Water disinfection using Kaolinite supported magnetic silver nanoparticle. *Chem. Data Collect.* **2022**, *39*, 100857. [[CrossRef](#)]

40. Jou, S.K.; Malek, N.A.N.N. Characterization and antibacterial activity of chlorhexidine loaded silver-kaolinite. *Appl. Clay Sci.* **2016**, *127–128*, 1–9. [[CrossRef](#)]
41. Zhang, X.; Zhang, J.; Qiu, L.; Lan, X.; Zhu, C.; Duan, J.; Liu, Y.; Li, H.; Yu, Y.; Yang, W. In-situ synthesis of dual Z-scheme heterojunctions of cuprous oxide/layered double hydroxides/nitrogen-rich graphitic carbon nitride for photocatalytic sterilization. *J. Colloid Interface Sci.* **2022**, *620*, 313–321. [[CrossRef](#)]
42. Wang, Q.; Yang, C.; Zhang, G.; Hu, L.; Wang, P. Photocatalytic Fe-doped TiO<sub>2</sub>/PSF composite UF membranes: Characterization and performance on BPA removal under visible-light irradiation. *Chem. Eng. J.* **2017**, *319*, 39–47. [[CrossRef](#)]
43. Li, R.; Cui, L.; Chen, M.; Huang, Y. Nanomaterials for airborne virus inactivation: A short review. *Aerosol Sci. Eng.* **2021**, *5*, 1–11. [[CrossRef](#)]
44. Chong, M.N.; Jin, B.; Saint, C.P. Bacterial inactivation kinetics of a photo-disinfection system using novel titania-impregnated kaolinite photocatalyst. *Chem. Eng. J.* **2011**, *171*, 16–23. [[CrossRef](#)]
45. Fatimah, I.; Hasanah, U.A.; Putra, H.P. Preparation of bifunctional ceramic membrane based on TiO<sub>2</sub>/kaolinite for water disinfection. *J. Mater. Environ. Sci.* **2014**, *5*, 1976–1981.
46. B.Aritonang, A.; Sapar, A.; Furqonita, A. Photocatalytic Bacterial Inactivation Using Bi-doped TiO<sub>2</sub>/Kaolinite Under Visible Light Irradiation. *Int. Conf. Sci. Eng.* **2021**, 105–111. [[CrossRef](#)]
47. Misra, A.J.; Das, S.; Rahman, A.P.H.; Das, B.; Jayabalan, R.; Behera, S.K.; Suar, M.; Tamhankar, A.J.; Mishra, A.; Lundborg, C.S.; et al. Doped ZnO nanoparticles impregnated on Kaolinite (Clay): A reusable nanocomposite for photocatalytic disinfection of multidrug resistant *Enterobacter* sp under visible light. *J. Colloid Interface Sci.* **2018**, *530*, 610–623. [[CrossRef](#)]
48. Pratap Reddy, M.; Venugopal, A.; Subrahmanyam, M. Hydroxyapatite-supported Ag–TiO<sub>2</sub> as *Escherichia coli* disinfection photocatalyst. *Water Res.* **2007**, *41*, 379–386. [[CrossRef](#)]
49. Ugwuja, C.G.; Adelowo, O.O.; Ogunlaja, A.; Omorogie, M.O.; Olukanni, O.D.; Ikhimiukor, O.O.; Iermak, I.; Kolawole, G.A.; Guenter, C.; Taubert, A.; et al. Visible-Light-Mediated Photodynamic Water Disinfection @ Bimetallic-Doped Hybrid Clay Nanocomposites. *ACS Appl. Mater. Interfaces* **2019**, *11*, 25483–25494. [[CrossRef](#)]
50. Kozera-Sucharda, B.; Gworek, B.; Kondzielski, I.; Chojnicki, J. The Comparison of the Efficacy of Natural and Synthetic Aluminosilicates, Including Zeolites, in Concurrent Elimination of Lead and Copper from Multi-Component Aqueous Solutions. *Processes* **2021**, *9*, 812. [[CrossRef](#)]
51. Hutchison, J.M.; Mayer, B.K.; Vega, M.; Chacha, W.E.; Zilles, J.L. Making Waves: Biocatalysis and Biosorption: Opportunities and Challenges Associated with a New Protein-Based Toolbox for Water and Wastewater Treatment. *Water Res. X* **2021**, *12*, 100112. [[CrossRef](#)]
52. Li, D.; Liu, S.-A.; Li, S. Copper isotope fractionation during adsorption onto kaolinite: Experimental approach and applications. *Chem. Geol.* **2015**, *396*, 74–82. [[CrossRef](#)]
53. Turan, P.; Doğan, M.; Alkan, M. Uptake of trivalent chromium ions from aqueous solutions using kaolinite. *J. Hazard. Mater.* **2007**, *148*, 56–63. [[CrossRef](#)] [[PubMed](#)]
54. Zhang, T.; Wang, W.; Zhao, Y.; Bai, H.; Wen, T.; Kang, S.; Song, G.; Song, S.; Komarneni, S. Removal of heavy metals and dyes by clay-based adsorbents: From natural clays to 1D and 2D nano-composites. *Chem. Eng. J.* **2021**, *420*, 127574. [[CrossRef](#)]
55. Yavuz, Ö.; Altunkaynak, Y.; Güzel, F. Removal of copper, nickel, cobalt and manganese from aqueous solution by kaolinite. *Water Res.* **2003**, *37*, 948–952. [[CrossRef](#)]
56. Et, A.; Shahmohammadi-Kalalagh, S. Isotherm and kinetic studies on adsorption of Pb, Zn and Cu by kaolinite. *Casp. J. Environ. Sci.* **2011**, *9*, 243–255.
57. Chai, W.; Huang, Y.; Su, S.; Han, G.; Liu, J.; Cao, Y. Adsorption behavior of Zn (II) onto natural minerals in wastewater. A comparative study of bentonite and kaolinite. *Physicochem. Probl. Miner. Process.* **2017**, *53*, 264–278. [[CrossRef](#)]
58. Farsi, A.; Aghasi, M.; Esmaeili, A.; Eslami, H. Efficient removal of Cu (II) and Zn (II) from aqueous solution and real acid mine drainage by natural vermiculite and kaolinite. *Desalin. Water Treat.* **2020**, *204*, 224–237. [[CrossRef](#)]
59. Novikau, R.; Lujanienė, G. Adsorption behaviour of pollutants: Heavy metals, radionuclides, organic pollutants, on clays and their minerals (raw, modified and treated): A review. *J. Environ. Manag.* **2022**, *309*, 114685. [[CrossRef](#)]
60. Yin, H.; Han, M.; Tang, W. Phosphorus sorption and supply from eutrophic lake sediment amended with thermally-treated calcium-rich attapulgite and a safety evaluation. *Chem. Eng. J.* **2016**, *285*, 671–678. [[CrossRef](#)]
61. Davidovits, J.; Sawyer, J.L. *Early High-Strength Mineral Polymer*; U.S. Patent and Trademark Office: Washington, DC, USA, 1985.
62. Yan, Z.; Fu, L.; Yang, H. Functionalized 2D clay derivative: Hybrid nanosheets with unique lead sorption behaviors and interface structure. *Adv. Mater. Interfaces* **2018**, *5*, 1700934. [[CrossRef](#)]
63. Krupskaya, V.; Novikova, L.; Tyupina, E.; Belousov, P.; Dorzhieva, O.; Zakusin, S.; Kim, K.; Roessner, F.; Badetti, E.; Brunelli, A. The influence of acid modification on the structure of montmorillonites and surface properties of bentonites. *Appl. Clay Sci.* **2019**, *172*, 1–10. [[CrossRef](#)]
64. España, V.A.A.; Sarkar, B.; Biswas, B.; Rusmin, R.; Naidu, R. Environmental applications of thermally modified and acid activated clay minerals: Current status of the art. *Environ. Technol. Innov.* **2019**, *13*, 383–397. [[CrossRef](#)]
65. Bhattacharyya, K.G.; Gupta, S.S. Removal of Cu (II) by natural and acid-activated clays: An insight of adsorption isotherm, kinetic and thermodynamics. *Desalination* **2011**, *272*, 66–75. [[CrossRef](#)]

66. Chai, J.-B.; Au, P.-I.; Mubarak, N.M.; Khalid, M.; Ng, W.P.-Q.; Jagadish, P.; Walvekar, R.; Abdullah, E.C. Adsorption of heavy metal from industrial wastewater onto low-cost Malaysian kaolin clay-based adsorbent. *Environ. Sci. Pollut. Res.* **2020**, *27*, 13949–13962. [[CrossRef](#)]
67. Unuabonah, E.; Olu-Owolabi, B.; Adebawale, K. Competitive adsorption of metal ions onto goethite–humic acid-modified kaolinite clay. *Int. J. Environ. Sci. Technol.* **2016**, *13*, 1043–1054. [[CrossRef](#)]
68. Timofeeva, M.N.; Panchenko, V.N.; Volcho, K.P.; Zakusin, S.V.; Krupskaya, V.V.; Gil, A.; Mikhalchenko, O.S.; Vicente, M.A. Effect of acid modification of kaolin and metakaolin on Brønsted acidity and catalytic properties in the synthesis of octahydro-2H-chromen-4-ol from vanillin and isopulegol. *J. Mol. Catal. A Chem.* **2016**, *414*, 160–166. [[CrossRef](#)]
69. Abdallah, S. Remediation of Copper and Zinc from wastewater by modified clay in Asir region southwest of Saudi Arabia. *Open Geosci.* **2019**, *11*, 505–512. [[CrossRef](#)]
70. Zhang, M.; Xia, M.; Li, D.; Sun, Z.; You, Y.; Dou, J. The effects of transitional metal element doping on the Cs (I) adsorption of kaolinite (001): A density functional theory study. *Appl. Surf. Sci.* **2021**, *547*, 149210. [[CrossRef](#)]
71. Üzüüm, Ç.; Shahwan, T.; Eroğlu, A.E.; Hallam, K.R.; Scott, T.B.; Lieberwirth, I. Synthesis and characterization of kaolinite-supported zero-valent iron nanoparticles and their application for the removal of aqueous Cu<sup>2+</sup> and Co<sup>2+</sup> ions. *Appl. Clay Sci.* **2009**, *43*, 172–181. [[CrossRef](#)]
72. Jiang, M.-Q.; Wang, Q.-P.; Jin, X.-Y.; Chen, Z.-L. Removal of Pb (II) from aqueous solution using modified and unmodified kaolinite clay. *J. Hazard. Mater.* **2009**, *170*, 332–339. [[CrossRef](#)]
73. Sari, A.; Tuzen, M. Cd (II) adsorption from aqueous solution by raw and modified kaolinite. *Appl. Clay Sci.* **2014**, *88*, 63–72. [[CrossRef](#)]
74. Egrani, D.; Latif, M.T.; Wessey, N.; Poyi, N.; Acharjee, S. Synthesis and characterization of kaolinite coated with copper oxide and its effect on the removal of aqueous Lead (II) ions. *Appl. Water Sci.* **2019**, *9*, 1–10. [[CrossRef](#)]
75. Abou-El-Sherbini, K.S.; Wahba, M.A.; Drweesh, E.A.; Akarish, A.I.; Shaban, S.A.; Elzahany, E.A. Zirconia-Intercalated Kaolinite: Synthesis, Characterization, and Evaluation of Metal-Ion Removal Activity. *Clays Clay Miner.* **2021**, *69*, 463–476. [[CrossRef](#)]
76. Tarasevich, Y.I.; Klimova, G. Complex-forming adsorbents based on kaolinite, aluminium oxide and polyphosphates for the extraction and concentration of heavy metal ions from water solutions. *Appl. Clay Sci.* **2001**, *19*, 95–101. [[CrossRef](#)]
77. Mao, S.; Gao, M. Functional organoclays for removal of heavy metal ions from water: A review. *J. Mol. Liq.* **2021**, *334*, 116143. [[CrossRef](#)]
78. Liu, P. Polymer modified clay minerals: A review. *Appl. Clay Sci.* **2007**, *38*, 64–76. [[CrossRef](#)]
79. Irandoost, M.; Pezeshki-Modaress, M.; Javanbakht, V. Removal of lead from aqueous solution with nanofibrous nanocomposite of polycaprolactone adsorbent modified by nanoclay and nanozeolite. *J. Water Process. Eng.* **2019**, *32*, 100981. [[CrossRef](#)]
80. Wang, A.; Chu, Y.; Muhmood, T.; Xia, M.; Xu, Y.; Yang, L.; Lei, W.; Wang, F. Adsorption properties of Pb<sup>2+</sup> by amino group's functionalized montmorillonite from aqueous solutions. *J. Chem. Eng. Data* **2018**, *63*, 2940–2949. [[CrossRef](#)]
81. Bhattacharyya, K.G.; Gupta, S.S. Kaolinite, montmorillonite, and their modified derivatives as adsorbents for removal of Cu (II) from aqueous solution. *Sep. Purif. Technol.* **2006**, *50*, 388–397. [[CrossRef](#)]
82. Unuabonah, E.; Adebawale, K.; Olu-Owolabi, B.; Yang, L. Comparison of sorption of Pb<sup>2+</sup> and Cd<sup>2+</sup> on kaolinite clay and polyvinyl alcohol-modified kaolinite clay. *Adsorption* **2008**, *14*, 791–803. [[CrossRef](#)]
83. Koteja, A.; Matusik, J. Di- and triethanolamine grafted kaolinites of different structural order as adsorbents of heavy metals. *J. Colloid Interface Sci.* **2015**, *455*, 83–92. [[CrossRef](#)] [[PubMed](#)]
84. Kočí, K.; Matějka, V.; Kovář, P.; Lacný, Z.; Obalová, L. Comparison of the pure TiO<sub>2</sub> and kaolinite/TiO<sub>2</sub> composite as catalyst for CO<sub>2</sub> photocatalytic reduction. *Catal. Today* **2011**, *161*, 105–109. [[CrossRef](#)]
85. Kang, S.; Hwang, J. CoMn<sub>2</sub>O<sub>4</sub> embedded hollow activated carbon nanofibers as a novel peroxymonosulfate activator. *Chem. Eng. J.* **2021**, *406*, 127158. [[CrossRef](#)]
86. Knížek, A.; Kubelík, P.; Bouša, M.; Ferus, M.; Civiš, S. Acidic Hydrogen Enhanced Photocatalytic Reduction of CO<sub>2</sub> on Planetary Surfaces. *ACS Earth Space Chem.* **2020**, *4*, 1001–1009. [[CrossRef](#)]
87. Chen, Y.; Wen, L.; Chen, J.; Luo, H.A.; Liu, J. In situ growth of g-C<sub>3</sub>N<sub>4</sub> on clay minerals of kaolinite, sepiolite, and talc for enhanced solar photocatalytic energy conversion. *Appl. Clay Sci.* **2022**, *216*, 106337. [[CrossRef](#)]
88. Schaefer, H.T.; Glezakou, V.A.; Owen, A.T.; Ramprasad, S.; Martin, P.F.; McGrail, B.P. Surface Condensation of CO<sub>2</sub> onto Kaolinite. *Environ. Sci. Technol. Lett.* **2013**, *1*, 142–145. [[CrossRef](#)]
89. Kadoura, A.; Narayanan Nair, A.K.; Sun, S. Adsorption of carbon dioxide, methane, and their mixture by montmorillonite in the presence of water. *Microporous Mesoporous Mater.* **2016**, *225*, 331–341. [[CrossRef](#)]
90. Hou, J.; Chen, M.; Zhou, Y.; Bian, L.; Dong, F.; Tang, Y.; Ni, Y.; Zhang, H. Regulating the effect of element doping on the CO<sub>2</sub> capture performance of kaolinite: A density functional theory study. *Appl. Surf. Sci.* **2020**, *512*, 145642. [[CrossRef](#)]
91. Li, R.; Rao, Y.; Huang, Y. Advances in catalytic elimination of atmospheric pollutants by two-dimensional transition metal oxides. *Chin. Chem. Lett.* **2022**, *12*, 108000. [[CrossRef](#)]
92. Liu, D.; Yuan, P.; Liu, H.; Li, T.; Tan, D.; Yuan, W.; He, H. High-pressure adsorption of methane on montmorillonite, kaolinite and illite. *Appl. Clay Sci.* **2013**, *85*, 25–30. [[CrossRef](#)]
93. Heller, R.; Zoback, M. Adsorption of methane and carbon dioxide on gas shale and pure mineral samples. *J. Unconv. Oil Gas Resour.* **2014**, *8*, 14–24. [[CrossRef](#)]

94. Deng, L.; Yuan, P.; Liu, D.; Annabi-Bergaya, F.; Zhou, J.; Chen, F.; Liu, Z. Effects of microstructure of clay minerals, montmorillonite, kaolinite and halloysite, on their benzene adsorption behaviors. *Appl. Clay Sci.* **2017**, *143*, 184–191. [[CrossRef](#)]
95. Lainé, J.; Foucaud, Y.; Bonilla-Petriciolet, A.; Badawi, M. Molecular picture of the adsorption of phenol, toluene, carbon dioxide and water on kaolinite basal surfaces. *Appl. Surf. Sci.* **2022**, *585*, 152699. [[CrossRef](#)]
96. Swasy, M.I.; Campbell, M.L.; Brummel, B.R.; Guerra, F.D.; Attia, M.F.; Smith, G.D.; Alexis, F.; Whitehead, D.C. Poly(amine) modified kaolinite clay for VOC capture. *Chemosphere* **2018**, *213*, 19–24. [[CrossRef](#)]
97. Mora, L.D.; Bonfim, L.F.; Barbosa, L.V.; da Silva, T.H.; Nassar, E.J.; Ciuffi, K.J.; Gonzalez, B.; Vicente, M.A.; Trujillano, R.; Rives, V.; et al. White and Red Brazilian Sao Simao's Kaolinite-TiO<sub>2</sub> Nanocomposites as Catalysts for Toluene Photodegradation from Aqueous Solutions. *Materials* **2019**, *12*, 3943. [[CrossRef](#)] [[PubMed](#)]
98. Kibanova, D.; Trejo, M.; Destailats, H.; Cervinisilva, J. Synthesis of hectorite-TiO<sub>2</sub> and kaolinite-TiO<sub>2</sub> nanocomposites with photocatalytic activity for the degradation of model air pollutants. *Appl. Clay Sci.* **2009**, *42*, 563–568. [[CrossRef](#)]
99. Yang, P.; Li, J.; Zuo, S. Promoting oxidative activity and stability of CeO<sub>2</sub> addition on the MnO<sub>x</sub> modified kaolin-based catalysts for catalytic combustion of benzene. *Chem. Eng. Sci.* **2017**, *162*, 218–226. [[CrossRef](#)]

**Disclaimer/Publisher's Note:** The statements, opinions and data contained in all publications are solely those of the individual author(s) and contributor(s) and not of MDPI and/or the editor(s). MDPI and/or the editor(s) disclaim responsibility for any injury to people or property resulting from any ideas, methods, instructions or products referred to in the content.